Thermodynamic stability and relaxation studies of small, triaza-macrocylic Mn(II) chelates

Arsénio de Sá[1], Célia S. Bonnet[2], Carlos F. G. C. Geraldes[3], Éva Tóth[2], Paula M.T. Ferreira[1*], João P. André[1*]

[1] Centro de Química, Campus de Gualtar, Universidade do Minho, 4710-057 Braga, Portugal

[2] Centre de Biophysique Moléculaire, CNRS, rue Charles Sadron, 45071, Orléans, France

[3] Departamento de Ciências da Vida, Faculdade de Ciências e Tecnologia, Centro de Neurociências e Biologia Celular and Centro de Química de Coimbra, Universidade de Coimbra, 3001-401 Coimbra, Portugal

*Corresponding author: Tel: +351 253 604 385; Fax: +351 253 604 382; Email: jandre@quimica.uminho.pt

Keywords: triaza, amphiphilic, manganese, MRI

Abstract

Due to its favorable relaxometric properties, Mn^{2+} is an appealing metal ion for magnetic resonance imaging (MRI) contrast agents. This paper reports the synthesis and characterization of three new triazadicarboxylate-type ligands and their Mn^{2+} chelates (**NODAHep**, 1,4,7-triazacyclononane-1,4-diacetate-7-heptanil; **NODABA**, 1,4,7-triazacyclononane-1,4-diacetate-7-benzoic acid; and **NODAHA** (1,4,7-

triazacyclononane-1,4-diacetate-7-hexanoic acid). The protonation constants of the ligands and the stability constants of the chelates formed with Mn^{2+} and the endogenous Zn^{2+} ion have been determined by potentiometry. In overall, the thermodynamic stability of the chelates is lower than that of the corresponding NOTA analogues (NOTA = 1,4,7-triazacyclononane-1,4,7-triacetate), consistent with the decreased number of coordinating carboxylate groups. Variable temperature ^{1}H NMRD and ^{17}O NMR measurements have been performed on the paramagnetic chelates to provide information on the water exchange rates and the rotational dynamics. The values of the ^{17}O chemical shifts are consistent with the presence of one water molecule in the first coordination sphere of Mn^{2+}. The three complexes are in the slow to intermediate regime for the water exchange rate, and they all display relatively high rotational correlation times, which explain the relaxivity values between 4.7 and 5.8 $mM^{-1}.s^{-1}$ (20 MHz and 298 K). These relaxivities are higher than expected for Mn^{2+} chelates of such size and comparable to those of small monohydrated Gd^{3+} complexes. The amphiphilic **[Mn(NODAHep)]** forms micelles above 22 mM (its critical micellar concentration was determined by relaxometry and fluorescence), and interacts with HSA via its alkylic carbon chain providing a 60% relaxivity increase at 20 MHz due to a longer tumbling time.

Introduction

Magnetic Resonance Imaging (MRI) has become one of the most successful diagnostic imaging modalities of the last decades. A large number of MRI scans is based on the use of paramagnetic contrast agents (CAs) which enhance the contrast of images of organs and tissues. Paramagnetic metal ions such as Gd^{3+} and Mn^{2+} are adequate for the preparation of CAs due to their high magnetic moment, long electronic relaxation times

and the lability of their coordinated water molecules. MRI contrast agents act by increasing both longitudinal ($1/T_1$) and transverse ($1/T_2$) relaxation rates of water protons in the human body, and their efficiency is expressed by their water proton relaxivity, r_i (i = 1,2) [1].

Thanks to its seven unpaired electrons and long electronic relaxation time, Gd^{3+} is the most widely used paramagnetic metal ion in MRI. To prevent toxicity, Gd^{3+} has to be administered to the patient in the form of a thermodynamically and kinetically stable chelate. Several gadolinium-based chelates have been approved as CAs, including Magnevist® ($[Gd(DTPA)]^-$, DTPA = diethylenetriaminepentaacetate) [2] or Dotarem® ($[Gd(DOTA)]^-$, DOTA = 1,4,7,10-tetraazacyclododecane-1,4,7,10-tetraacetate) [3].

Despite its favorable features (five unpaired *d* electrons, long electronic relaxation times and labile coordinated water molecule(s)), Mn^{2+} received less attention and there has been only one approved Mn^{2+}-based contrast agent (Teslascan®, $[MnDPDP]^{4-}$, $DPDP^{6-}$ = *N*,*N*'-dipyridoxylethylenediamine-*N*,*N*'-diacetate-5,5'-bis-(phosphate), Scheme 1) [4, 5]. A renewed interest in Mn^{2+}-based MRI CAs has led to a systematic development and study of Mn^{2+} chelates [6]. These include linear polyaminocarboxylates like EDTA [7, 8] (EDTA = ethylenediamine tetraacetic acid) and its derivatives such as EDTA-$BOM_{1,2}$ [9] and diphEDTA [10] (bearing one or two BOM = benzyloxymethyl or a diph = diphenylcyclohexylphosphate substituent(s), respectively), or derivatives of DTPA [10-13] (DTPA = diethylenetriamine pentaacetic acid). In these EDTA-type complexes, the Mn^{2+} ion has a coordination number CN of 7 with one inner sphere coordinated water molecule. Chelates of Mn^{2+} with macrocyclic polyamino-polycarboxylate ligands which have been described include derivatives of triazacyclononane (NOTA [14] (NOTA = 1,4,7-triazacyclononane-1,4,7-triacetic acid) and the dimeric ENOTA [15]), of diaza-oxacyclononane (9-aneN_2O derivatives [16]), of tetraazacyclononane (DOTA [14]) and its

derivatives bearing four or less pendant arms [9, 17, 18], such as DOTAM (DOTAM = 1,4,7,10-tetraazacyclododecane-1,4,7,10-tetraacetamide), ($DO3A(BOM)_3$ (DO3A = 1,4,7,10-tetraazacyclododecane-1,4,7-triacetic acid, BOM = benzyloxymethyl) and DO2A = 1,4,7,10-tetraazacyclododecan-1,7-diacetic acid), and a 1,4-diazepine-based ligand (AAZTA = 6-amino-6-methylperhydro-1,4-diazepine triacetic acid) [19]. The Mn^{2+} complexes of these ligands have a maximum of one water molecule on the first coordination sphere, and the DOTA, DOTAM and $DO3A(BOM)_3$ complexes have no inner-sphere water. Bishydrated Mn^{2+} complexes have been reported with ligands based on 15- or larger membered aza- or aza-oxa crown ethers containing five donor atoms, of which one could be in a pyridine moiety (py), *e.g.* 15-aneN5 [20], Me_2-15-pydieneN_5 [21], 15-pyN_5 or 15-pyN_3O_2 [22].

In the development of novel and better MRI contrast agents, two main goals are commonly considered: higher relaxivity and specificity for organs or tissues. Human serum albumin (HSA), the most abundant blood serum protein, presenting high affinity for long carbon chain molecules, [23] is an interesting biological target for CAs, especially those aimed at acting as blood pool agents. Chelates bearing hydrophobic moieties can bind to HSA, thus increasing their blood retention time and, simultaneously, increasing their relaxivity due to longer tumbling times [9, 24-26].

Several strategies have been suggested for the delivery of drugs, among them self-aggregating molecules that can form micelles [27-29]. This delivery route is known to be promoted by macrophage-rich tissues such as liver and spleen [30]. Micellization of amphiphilic paramagnetic chelates has the additional advantage of increasing the relaxivity thanks to an increase in the tumbling time of the chelate in solution [31-36]. Another strategy for the development of CAs targeted for specific tissues and organs consists in their coupling to biologically relevant molecules (monoclonal antibodies,

peptides, peptide mimetics or non-peptidic substrates and carbohydrates [37-42]) that are recognized by specific receptors.

In this paper, we report the synthesis of three new triazapolycarboxylate-based ligands for Mn^{2+}, **NODAHep** (1,4,7-triazacyclononane-1,4-diacetate-7-heptanil), **NODABA** (1,4,7-triazacyclononane-1,4-diacetate-7-benzoic acid), and **NODAHA** (1,4,7-triazacyclononane-1,4-diacetate-7-hexanoic acid) (Scheme 1) and the solution characterization of the stability and relaxometric properties of their Mn^{2+} complexes using potentiometric and relaxometric NMR techniques. Being pentadentate, these ligands maintain a coordination site of the metal ion available for one water molecule. **NODAHep** has a lipophilic side chain which was introduced to endow its chelates with the capability of forming micelles in solution and, additionally, to interact non-covalently with blood serum proteins, in particular HSA. **NODABA** and **NODAHA** were designed to act as bifunctional ligands which can be conjugated to targeting molecules.

Results and discussion

Synthesis

The synthetic strategy used for the preparation of **NODAHep**, **NODABA** and **NODAHA** involved the alkylation of 1,4,7-triazacyclononane-1,4-diacetic acid *tert*-butyl ester (NO2AtBu) followed by removal of the protecting groups (Scheme 2). In the case of **NODAHep**, 1-bromoheptane was reacted with NO2AtBu in the presence of potassium carbonate to give **NODA(^{t}Bu)Hep**. This compound was then treated with trifluoroacetic acid (TFA) to give **NODAHep** in a 78% yield. The synthesis of **NODABA** and **NODAHA** was carried out using as alkylating agents the 9-fluorenylmethyl ester of 4-(bromomethyl)benzoic acid and the methyl ester of 6-

bromohexanoic acid to give **NODA(^{t}Bu)BA** and **NODA(^{t}Bu)HA(me)** in high yields. The **NODABA** and **NODAHA** were obtained by treating **NODA(^{t}Bu)BA** with trifluoracetic acid and **NODA(^{t}Bu)HA(me)** with a solution of NaOH. The unprotected carboxylic acid present in **NODABA** and **NODAHA** can be used to link a vectorizing moiety.

The preparation of the Mn(II) chelates was done in HEPES buffer pH 7.4. The formation of the chelates occurred rapidly.

Determination of the critical micelle concentration

The critical micelle concentration (cmc) of **[Mn(NODAHep)]** was determined by two methods. In the first method a fluorescence probe was used, which was 8-anilino-1-naphtalene sulfonic acid (ANS), as its luminescence is sensitive to the medium polarity. In polar environments, such as in water, ANS is essentially non fluorescent and in non-polar environments, such as the inner part of micelles, it is highly fluorescent [43-45]. In order to evaluate the micelles formation, the fluorescence intensity of ANS was measured at 480 nm in the presence of different chelate concentrations. As the micelles are forming, ANS is entrapped in the micellar compartment and an increase of its fluorescence can be detected [44, 45]. A cmc value of 22.3 mM was determined by linear least-square fitting of the fluorescence emission at 480 nm versus the concentration of the **[Mn(NODAHep)]** chelate (Figure 1). The alternative method consisted in the measurement of the longitudinal relaxation rate of the water hydrogen nuclei with increasing concentrations of **[Mn(NODAHep)],** at 40 MHz and 298 K. Indeed, at concentrations below the cmc, no micelles are formed, and therefore the proton relaxation rate measured in the solution is only due to the free, non-aggregated paramagnetic complex and can be expressed as follows:

$$R_1 = r_1^{na} C_{Mn} \qquad (1)$$

where R_1 is the paramagnetic relaxation enhancement, r_1^{na} is the relaxivity of the non-aggregated Mn^{2+} complex, and C_{Mn} is the Mn^{2+} concentration. Above the cmc, the measured relaxation rate is the sum of two contributions, one from the non-aggregated complex present at a concentration equal to the cmc, and one of the complex in the micellar form. The paramagnetic relaxation enhancement in this case is given by:

$$R_1 = r_1^{na} \times cmc + r_1^{a}(C_{Mn} - cmc) = (r_1^{na} - r_1^{a})cmc + r_1^{a} C_{Mn} \qquad (2)$$

where r_1^{a} is the relaxivity of the aggregated form of the complex.

The cmc is then determined from the plot of R_1 as a function of C_{Mn}, and by a simultaneous least-squares fit of the two straight lines. The intercept of those two lines gives the value of the cmc, 22.8 mM in this case (Figure S1), very much consistent with the result obtained in the previous method. It should be noted that the relaxivity of the non-aggregated form is found to be 4.51 $mM^{-1}.s^{-1}$ in accordance with the ^1H NMRD measurements (vide infra), and the relaxivity of the micellar form is found to be 9.57 $mM^{-1}.s^{-1}$. This higher value of relaxivity was predictable, as in the micellar form the rotational correlation time is expected to be bigger than in the monomeric form.

The cmc values obtained for **[Mn(NODAHep)]** are higher than those found for complexes such as [Ga(NOTAC8)] and [Al(NOTAC8)], 0.36 mM and 0.25 mM respectively (NOTAC8 = 1,4,7-triazacyclononane-1,4-diacetic acid-7-octanoic acid (Scheme 1) [46]. This is somewhat surprising, considering that **NODAHep** and NOTAC8 have the same length of alkyl chain, and the three complexes have no charge. Given the

high value of cmc obtained for this complex, we will study only the monomeric form of the complex in the followings.

Determination of protonation and stability constants

The protonation constants, logK_{Hi}, of the three ligands **NODAHep**, **NODAHA** and **NODABA**, as defined in equation (3), were determined by pH-potentiometric titrations at I = 0.1 M KCl and 298 K.

$$K_{H_i} = \frac{[H_iL]}{[H_{i-1}L][H^+]} \qquad (3)$$

Three protonation constants could be determined for **NODAHep,** four for **NODAHA** and five for **NODABA**. The titration curves are presented in Figures 2 and S2, S3 (ESI) and the calculated protonation constants are shown in Table 1.

The potentiometric determination of protonation constants above pH 11 is difficult, and they can be assessed by ^{1}H NMR spectroscopy if the chemical shifts of the non-labile protons of the ligand exhibit a chemical shift change upon deprotonation. However in our case, attempts to determine these protonation constants by NMR were unsuccessful as the chemical shift changes observed were of the same order of magnitude as the line broadening of the observed peaks. For this reason the values obtained from potentiometric titrations, with a large error taking into account the difficulty of their determination, have been considered.

The protonation sequence has been previously determined for various cyclic polyaza polycarboxylate ligands, and it has been shown that the first two protonations of the ligand NOTA occur on the ring nitrogen atoms, while the third protonation occur on a carboxylate oxygen atom [47]. So for all the ligands, we attribute the first two protonation constants to two nitrogen atoms of the macrocycle, and the other protonation constants

are attributed to carboxylate functions. **NODAHep** is very similar to "half" ENOTA (Scheme 1), which displays two macrocyclic units. And indeed, the protonation constants of **NODAHep** are very close to those obtained for ENOTA (12.5, 12.2, 5.97, 5.18, 2.73, 1.86) [15]. For **NODAHA**, the third protonation constant can be attributed to the carboxylate function on the alkyl chain, as the value is close to the one of an isolated carboxylate function. For **NODABA**, the second protonation on the nitrogen is lower than the one of the other ligand, which can be explained by the electron withdrawing effect of the benzene ring. The third protonation constant can be attributed to the benzoate function, as the pKa of the benzoic acid substituted in the *para* position by a methyl is 4.37 [48].

Complex stability constants, $\log K_{ML}$, complex protonation constants, $\log K_{MLH}$, and hydroxo-complexes formation (eqs (4), (5), and (6)), have been determined for complexes formed with Mn^{2+} and Zn^{2+} ions by direct potentiometric titrations, as the formation of the complexes was fast.

$$K_{ML} = \frac{[ML]}{[M][L]} \qquad (4)$$

$$K_{MLH} = \frac{[MLH]}{[H][ML]} \qquad (5)$$

$$K_{ML(OH)} = \frac{[ML]}{[ML(OH)][H]} \qquad (6)$$

The titration curves obtained at 1:1 metal-to-ligand ratio are presented in Figures 2 and S2, S3 (ESI). The stability constants obtained from the fitting of the experimental curves for the different complexes are summarized in Table 2.

The formation of a monoprotonated complex and a hydroxocomplex has to be taken into account for **NODAHA**. The stability constants obtained for the Mn^{2+} complexes are similar for the three ligands and they are 5 to 6 orders of magnitude lower than the one obtained with Zn^{2+}. In order to compare the thermodynamic stability of these complexes with those from the literature, we calculated the pMn values for conditions commonly used for Gd^{3+} chelates (pH = 7.4, $[Mn^{2+}] = 10^{-6}$ M, [L] = 10^{-5} M). The values are similar for the three complexes, and they are also similar to the one found for the binuclear ENOTA complex (pM = 7.7) [15]. They are also in the same order of magnitude as the one found for pyridine-containing macrocyclic ligands with carboxylate, or phosphate as pendants arms [22, 50], or the ones of 9-aneN_2O [16] ligands with similar pendant arms. They however remain 4 to 5 orders of magnitude lower than those of MnNOTA, or MnEDTA, and 7 orders of magnitude lower than the pMn of DOTA [51].

^{17}O NMR and NMRD measurements

In order to determine the microscopic parameters that rule the relaxivity of the complexes, their ^{1}H NMRD profiles have been measured. These profiles represent the magnetic field dependence of relaxivity on the proton Larmor precession frequency and can be fitted by the Solomon-Bloembergen-Morgan (SBM) theory. As a large number of microscopic parameters influence the ^{1}H NMRD profiles, some of them need to be determined by independent techniques such as ^{17}O NMR. The variable-temperature ^{17}O transverse relaxation rates ($1/T_2$) give access to the exchange rate of the Mn^{2+}-coordinated water molecule, k_{ex}; the longitudinal relaxation rates ($1/T_1$) provide information about the rotational motion of the complex, and hence τ_R, and finally the ^{17}O chemical shifts (ω) inform about the hydration number (q) of the complex.

The transverse ^{17}O relaxation times were measured as a function of temperature on aqueous solutions of the three complexes. The longitudinal relaxation times were also

measured but were not included in the fittings as the difference between the paramagnetic solution and the diamagnetic reference were too small to yield reliable values. The chemical shifts were also measured but the differences in the chemical shifts were too small compared to the line broadening of the peak to be included in the treatment of the data.

The ^{17}O transverse relaxation rates and the ^{1}H NMRD data at 298, 310, and 323 K (Figures 3 and S4, S5) were analysed simultaneously with the SBM theory to yield the microscopic parameters of the complexes characterizing water exchange and rotation (see ESI for equations). As can be seen in the figures, the ^{17}O reduced transverse relaxation rates ($1/T_{2r}$) first increase and then slightly decrease with increasing temperature, indicating that the complexes are mainly in the slow to intermediate exchange regime. In the slow kinetic region, $1/T_{2r}$ is directly determined by the exchange rate k_{ex}. At higher temperature, $1/T_{2r}$ is defined by the transverse relaxation rate of the bound water oxygen, $1/T_{2m}$, which in turn is influenced by the water exchange rate, k_{ex}, the longitudinal electronic relaxation rate, $1/T_{1e}$, and the scalar coupling constant, $A/\hbar$. The transverse ^{17}O relaxation is governed by the scalar relaxation mechanism and thus contains no information on the rotational motion of the system. If we are not interested in detailed information about the electron spin relaxation and if we restrict the analysis of the NMRD data to medium and high magnetic fields, the SBM approach gives reliable information on dynamic processes like water exchange and rotational correlation times for small complexes [52]. Therefore only relaxivity values above 6 MHz have been included in the simultaneous fit and the following parameters have been thus adjusted: the water exchange rate, k_{ex}^{298}, the activation enthalpy for water exchange, $\Delta H^{\neq}$, the scalar coupling constant, $A/\hbar$, the rotational correlation time, τ_R^{298}, and its activation energy, E_R, and the parameters

describing electron spin relaxation, the mean square of the zero field splitting, Δ^2, the correlation time for the modulation of the zero field splitting, τ_V^{298}, while its activation energy, $E_{V,}$ has been fixed to 20 kJ/mol. The diffusion coefficient D_{GdH}^{298}, and its activation energy E_{DGdH} were fixed to 23×10^{-10} m^2s^{-1} and 20 $kJmol^{-1}$, respectively. The distances between the Mn^{2+} ion and the inner and the outer sphere water protons were fixed to r_{MnH} = 2.75 Å and a_{MnH} = 3.2 Å, respectively. The parameters resulting from the best fit are presented in Table 3. As **[Mn(NODABA)]** is clearly in the slow exchange region, no information on the electronic parameters of these complexes can be obtained from the ^{17}O T_2 values. Therefore, for the analysis of this system, we decided to fix the electronic parameters to the values obtained from the fittings of the two other complexes.

The exchange rate of the complexes are of the same order of magnitude as that of the aqua ion and slightly lower than the one of the dinuclear complex ENOTA. The negative values of the activation entropy tend to point to an associative mechanism for the exchange rate of the water molecule, as demonstrated for the Mn_2ENOTA. The six-coordinated monohydrated complexes will undergo an associative exchange which proceeds via a seven-coordinate transition state. **[Mn(NODAHep)]** and **[Mn(NODABA)]** are certainly six-coordinated species with one water molecule in the first coordination sphere of Mn^{2+}. In the case of **[Mn(NODAHA)],** the carboxylate function on the alkyl chain could also participate in the coordination sphere of Mn^{2+}. Given the species found from potentiometric measurements (presence of a protonated complex) and the results obtained from the activation entropy, we can conclude that the carboxylate function on the alkyl chain of **NODAHA** does not participate in the coordination sphere of the metal ion. The slower water exchange observed for **[Mn(NODABA)]** can be explained by the presence of the bulky benzyl ring, which

does not facilitate the approach of the second water molecule in the water exchange mechanism. The scalar coupling constants found are typical of a Mn^{2+} complex [16, 22], confirming the monohydrated character of the complex.

The ^1H NMRD profiles are comparable to those of Mn(EDTA) and other monohydrated Mn^{2+} complexes. No second dispersion is observed at low field, unlike what has been observed for the dinuclear Mn_2ENOTA complex. This absence of second dispersion moreover confirms the absence of free Mn^{2+}. The relaxivities of **[Mn(NODAHep)]**, **[Mn(NODAHA)]** and **[Mn(NODABA)]** at 20 MHz and 298 K are respectively 4.73, 4.58 and 5.47 $mM^{-1}.s^{-1}$, remarkably higher than that of the similarly monohydrated Mn(EDTA) (3.0 at 24 MHz, 298 K) [54]. This difference can be accounted for by the larger size of our complexes. The slightly higher value observed for **[Mn(NODABA)]** can be explained by the higher rotational correlation time of the complex.

These relaxivities are similar to those of Gd^{3+} chelates with one water molecule in the first coordination sphere of the metal ion (GdDOTA: r_1 = 4.2 $mM^{-1}.s^{-1}$; GdDTPA: r_1 = 4.3 $mM^{-1}.s^{-1}$) [41]. In general, considering chelates of similar size, Gd^{3+} complexes have higher relaxivities because of the higher electron spin of Gd^{3+} with respect to Mn^{2+}. A general feature of Mn^{2+} complexes with respect to the Gd^{3+} analogues is their faster water exchange which can be advantageous to attain high relaxivities, but only for slowly rotating systems.

We have also measured the NMRD profile of **[Mn(NODAHep)]** in the presence of HSA (Figure S6 in ESI). Given the hydrophobic nature of the alkyl chain, non-covalent binding between the complex and the protein through hydrophobic interactions is expected as it was reported for various Gd^{3+}- [55] and some Mn^{2+}-chelates [9, 10]. Indeed, the NMRD curve displays a “hump” between 10 and 80 MHz, typical of slowly rotating complexes (at 20 MHz, the relaxivity is nearly doubled in the presence of HSA)

confirming that the complex is bound to HSA through hydrophobic interaction. We should note that this interaction is certainly not specific to HSA, but would be operative for many other proteins as well.

pH stability

The stability of **[Mn(NODAHep)]** was also investigated as a function of the pH. The increase of relaxivity observed upon going from basic to acidic pH can be attributed to the decomplexation of Mn^{2+} ion at acidic pH, lower than 5. This is indeed in accordance with the species distribution obtained from the stability constant of **[Mn(NODAHep)]** determined by potentiometry (Figure 4). We can conclude that in the pH range 7.4 - 9.3, the complex is formed.

Conclusions

In this paper we introduce three new chelators designed for Mn^{2+} as potential MRI CAs. The protonation constants and the thermodynamic stabilities of their Mn^{2+} and Zn^{2+} chelates have been determined by pH potentiometry. The thermodynamic stability constants are lower in comparison to those of the analogous NOTA chelates. The parameters governing relaxivity have been obtained by ^{1}H NMRD and ^{17}O NMR studies. They are compatible with small molecular weight chelates displaying one inner sphere water molecule that exchanges via an associative water exchange mechanism. The Mn^{2+} chelates display relaxivities between 4.6 and 5.5 $mM^{-1}.s^{-1}$ (20 MHz and 298 K), values which are similar to those of monohydrated Gd^{3+} chelates. The slightly higher relaxivity value found for **[Mn(NODABA)]** is explained by a longer rotational correlation time.

The alkylic pendant chain of **NODAHep** endows its Mn^{2+} chelate with amphiphilic character, forming micelles in solution. Its cmc has been determined by two distinct

methods, affording similar values (22.3 mM by fluorescence and 22.8 mM by relaxivity). Simultaneously the alkylic chain permits the chelate to interact with HSA, resulting in a 60% relaxivity increase (at concentrations similar to those present in the blood, 4% (0.6 mM) [56]) due to an even longer tumbling time. It is also expected that the interaction with HSA might increase the retention time of the chelate in the blood stream.

Experimental

Materials and methods

Analytical grade reagents were purchased from Sigma-Aldrich, Fluka, Acros Organics, Macrocyclics and Chematech. The reactions were monitored by thin layer chromatography (TLC) on aluminum plates coated with silica gel 60 F_{254} (Macherey-Nagel). Chromatography separations were performed on silica gel Whatman 230-240 Mesh. The NMR spectra were recorded on a Varian Unity Plus 300 spectrometer or on a BrukerAvance III 400 spectrometer. The ^{1}H NMR spectra were assigned using the two-dimensional COSY technique. The ^{1}H chemical shifts are reported in ppm, relative to tetramethylsilane (TMS) or sodium 2,2-dimethylsilapentane-5-sulfonate (DSS) and the following abbreviations are used: s = singlet; d = duplet; t = triplet; m = multiplet. pH measurements were performed on a pH meter Crison micro TT 2050 with an electrode Mettler Toledo InLab 422. Mass spectra (ESI^+) were performed on a VG Autospec M spectrometer or on a Finnigan LXQ MS Detector.

Synthetic procedures

NODA(^{t}Bu)Hep

To a solution of NO2AtBu (0.520 g, 1.45 mmol) in acetonitrile (22 mL), K_2CO_3 (0.606 g, 4.38 mmol) and 1-bromoheptane (0.230 mL, 1.46 mmol) were added. The reaction

was stirred for 96 h. The reaction mixture was filtered and the solvent removed under reduced pressure. The oil obtained was purified by column chromatography using dichloromethane/ethanol 7:3 and dichloromethane/ethanol/NH_3 7:3:0.5. The **NODA(^{t}Bu)Hep** (0.660 g, 1.45 mmol) was obtained as an oil with 100% yield. δ_H (300 MHz; $CDCl_3$; TMS) 0.85 (3 H, t, *J* = 6.8 Hz, $(CH_2)_6CH_3$), 1.24 (8 H, m, $(CH_2)_6CH_3$), 1.43 (20 H, m, $(CH_2)_6CH_3$ and $C(CH_3)_3$), 2.48 (2 H, t, *J* = 7.8 Hz, $(CH_2)_6CH_3$), 2.70-2.90 (12 H, m, *en*) and 3.29 (4 H, s, $CH_2CO_2{}^t$Bu). δ_C (100.61 MHz; $CDCl_3$; TMS) 14.02 ($(CH_2)_6CH_3$), 22.56 ($(CH_2)_6CH_3$), 27.42 ($(CH_2)_6CH_3$), 28.16 ($C(CH_3)_3$), 29.18 ($(CH_2)_6CH_3$), 31.79 ($(CH_2)_6CH_3$), 55.20 (*en*), 58.61 ($(CH_2)_6CH_3$), 59.73 ($CH_2CO_2{}^t$Bu), 80.65 ($C(CH_3)_3$) and 171.46 ($CH_2CO_2{}^t$Bu). HRMS (ESI^+) calculated for $C_{25}H_{50}N_3O_4$ $(M+H)^+$ 456.38013. Found 456.37890.

NODAHep

Trifluoracetic acid (30 mL) was added to a solution of **NODA(^{t}Bu)Hep** (0.660 g, 1.45 mmol) in dichloromethane (30 mL). The mixture was left stirring at room temperature overnight. The solvent was removed under reduced pressure and the oil obtained was washed with hexane (3 x 15 mL) and water (3 x 15 mL). The **NODAHep** (0.775 g, 1.13 mmol) was obtained as an oil with 78% yield. δ_H (300 MHz; D_2O; DSS) 0.84 (3 H, t, *J* = 6.8 Hz, $(CH_2)_6CH_3$), 1.20-1.40 (8 H, m, $(CH_2)_6CH_3$), 1.72-1.82 (2 H, m, $(CH_2)_6CH_3$), 3.28-3.65 (14 H, m, $(CH_2)_6CH_3$ and *en*) and 3.86 (4 H, s, CH_2CO_2H). δ_C (75.43 MHz; D_2O; DSS) 13.46 ($(CH_2)_6CH_3$), 22.00 ($(CH_2)_6CH_3$), 23.80 ($(CH_2)_6CH_3$), 25.78 ($(CH_2)_6CH_3$), 27.98 ($(CH_2)_6CH_3$), 30.92 ($(CH_2)_6CH_3$), 49.57 (*en*), 50.68 (*en*), 50.92 (*en*), 57.06 (CH_2CO_2H), 58.29 ($(CH_2)_6CH_3$) and 173.29 (CH_2CO_2H). HRMS (ESI^+) calculated for $C_{17}H_{34}N_3O_4$ $(M+H)^+$ 344.25493. Found 344.25378.

9-Fluorenylmethyl 4-(bromomethyl)benzoate

N,*N*′-dicyclohexylcarbodiimide (0.484 g, 2.34 mmol) and 4-(dimethylamino)pyridine (0.015 g, 0.123 mmol) were added to a solution of 4-(bromomethyl)benzoic acid (0.505 g, 2.35 mmol) and 9-fluorenemethanol (0.508 g, 2.59 mmol) in dry dichloromethane (15 mL) in ice bath. The reaction was stirred, at room temperature, for 72 h. The reaction mixture was filtered and the solvent removed under reduced pressure. The residue obtained was purified by column chromatography eluted using cyclohexane/ethyl acetate 4:1. The **9-fluorenylmethyl 4-(bromomethyl)benzoate** (0.436 g, 1.15 mmol) was obtained as an oil with 49% yield. δ_H (400 MHz; $CDCl_3$; TMS) 4.40 (1 H, t, *J* = 7.2 Hz, *Fm*), 4.53 (2 H, s, $C_6H_4CH_2Br$), 4.64 (2 H, d, *J* = 7.2 Hz, *Fm*), 7.34 (2 H, t, *J* = 7.6 Hz, *Fm*), 7.44 (2 H, t, *J* = 7.4 Hz, *Fm*), 7.52 (2 H, d, *J* = 7.8 Hz, $C_6H_4CH_2Br$), 7.66 (2 H, t, *J* = 7.6 Hz, *Fm*), 7.81 (2 H, t, *J* = 7.6 Hz, *Fm*) and 8.07 (2 H, d, *J* = 7.8 Hz, $C_6H_4CO_2Fm$). δ_C (100.61 MHz; $CDCl_3$; TMS) 32.15 ($PhCH_2Br$), 46.91 (CH_2CH *Fm*), 67.12 (CH_2CH *Fm*), 120.08 (*Fm*), 125.02 (*Fm*), 127.17 (*Fm*), 127.85 (*Fm*), 129.18 ($C_6H_4CH_2Br$), 130.01 ($C_6H_4CH_2Br$), 130.11 ($C_6H_4CH_2Br$), 141.34 (*Fm*), 142.82 ($C_6H_4CH_2Br$), 143.73 (*Fm*) and 165.90 ($PhCO_2Fm$).

NODA(^{t}Bu)BA

To a solution of NO2AtBu (0.301 g, 0.842 mmol) in acetonitrile (20 mL), K_2CO_3 (0.472 g, 3.42 mmol) and 9-fluorenylmethyl 4-(bromomethyl)benzoate (0.318 g, 0.838 mmol) were added. The reaction was stirred for several days. The reaction mixture was filtered and the solvent removed under reduced pressure. The oil obtained was purified by column chromatography eluted using ethyl acetate/ethanol 1:1, ethanol and ethanol/NH_3 10:0.5. **NODA(^{t}Bu)BA** (0.410 g, 0.834 mmol) was obtained as an oil in 99% yield. δ_H (300 MHz; $CDCl_3$; TMS) 1.42 (18 H, s, $C(CH_3)_3$), 2.79-3.47 (16 H, m, *en* and $CH_2CO_2{}^t$Bu), 4.23 (2 H, s, $CH_2C_6H_4CO_2H$), 7.50 (2 H, d, *J* = 7.8 Hz, $CH_2C_6H_4CO_2H$) and 8.02 (4 H, d, *J* = 8.1 Hz, CH_2 $C_6H_4CO_2H$). δ_C (75.43 MHz; $CDCl_3$; TMS) 28.10

(C(*C*H$_3$)$_3$), 51.68 (*en*), 52.43 (*en*), 55.00 (*en*), 59.47 (*C*H$_2$C$_6$H$_4$CO$_2$H and *C*H$_2$CO$_2$^{t}Bu), 81.24 (*C*(CH$_3$)$_3$), 129.74 (CH$_2$*C*$_6$H$_4$CO$_2$H), 129.93 (CH$_2$*C*$_6$H$_4$CO$_2$H), 135.52 (CH$_2$*C*$_6$H$_4$CO$_2$H), 136.55 (CH$_2$*C*$_6$H$_4$CO$_2$H), 170.73 (CH$_2$*C*O$_2$^{t}Bu) and 171.11 (CH$_2$C$_6$H$_4$*C*O$_2$H). HRMS (ESI$^+$) calculated for $C_{26}H_{42}N_3O_6$ $(M+H)^+$ 492.30736. Found 492.30612.

NODABA

Trifluoracetic acid (18 mL) was added to a solution of **NODA(*t*Bu)BA** (0.415 g, 0.844 mmol) in dichloromethane (18 mL). The mixture was left stirring overnight and solvent removed under reduced pressure. The oil obtained was washed with hexane (3 x 9 mL) and water (3 x 9 mL). **NODABA** (0.470 g, 0.651 mmol) was obtained in 77% yield, as an oil. δ_H (400 MHz; D_2O; DSS) 3.25-3.63 (12 H, m, *en*), 3.81 (4 H, s, C*H*$_2$CO$_2$H), 4.57 (2 H, s, C*H*$_2$C$_6$H$_4$CO$_2$H), 7.67 (2 H, d, *J* = 6.3 Hz, CH$_2$C$_6$*H*$_4$CO$_2$H) and 8.06 (2 H, d, *J* = 6.3 Hz, CH$_2$C$_6$*H*$_4$CO$_2$H). δ_C (100.6 MHz; D_2O; DSS) 49.36 (*en*), 50.31 (*en*), 50.74 (*en*), 56.32 (*C*H$_2$CO$_2$H), 60.37 (*C*H$_2$C$_6$H$_4$CO$_2$H), 130.50 (CH$_2$*C*$_6$H$_4$CO$_2$H), 131.28 (CH$_2$*C*$_6$H$_4$CO$_2$H), 131.44 (CH$_2$*C*$_6$H$_4$CO$_2$H), 134.13 (CH$_2$*C*$_6$H$_4$CO$_2$H), 169.53 (CH$_2$C$_6$H$_4$*C*O$_2$H) and 172.56 (CH$_2$*C*O$_2$H). HRMS (ESI$^+$) calculated for $C_{18}H_{26}N_3O_6$ $(M+H)^+$ 380.18216. Found 380.18152.

Methyl 6-bromohexanoate

Thionyl chloride (3.74 mL, 51.3 mmol) was slowly added to methanol (15 mL) in an ice bath. A solution of 6-bromohexanoic acid (2.002 g, 10.26 mmol) in 30 mL of methanol was added to the previous solution. The mixture was left stirring at 313 K for 4 h. The solvent was evaporated giving **methyl 6-bromohexanoate** (1.903 g, 9.10 mmol) in 89% yield as a solid. δ_H (300 MHz; $CDCl_3$; TMS) 1.46 (2 H, m, γC*H*$_2$), 1.65 (2 H, m, βC*H*$_2$), 1.86 (2 H, m, δC*H*$_2$), 2.32 (2 H, t, *J* = 7.5 Hz, αC*H*$_2$), 3.39 (2 H, t, *J* = 6.6 Hz, εC*H*$_2$) and 3.66 (3 H, s, C*H*$_3$).

NODA(^{t}Bu)HA(me)

K_2CO_3 (0.241 g, 1.741 mmol) and methyl 6-bromohexanoate (0.148 g, 0.707 mmol) were added to a solution of NO2AtBu (0.211 g, 0.589 mmol) in acetonitrile (15 mL). The reaction was stirred for 96 h. The reaction mixture was filtered and the solvent removed under reduced pressure. The oil obtained was purified by column chromatography eluted using dichloromethane/ethanol 7:3 and dichloromethane/ethanol/NH_3 7:3:0.5. The **NODA(^{t}Bu)HA(me)** (0.282 g, 0.581 mmol) was obtained with 99% yield, as an oil. δ_H (300 MHz; $CDCl_3$; TMS) 1.31 (2 H, m, γC*H*$_2$), 1.36 (18 H, s, C(C*H*$_3$)$_3$), 1.57 (4 H, m, βC*H*$_2$ and δC*H*$_2$), 2.25 (2 H, t, *J* = 7.2 Hz, αC*H*$_2$), 2.62-3.10 (14 H, m, εC*H*$_2$ and *en*), 3.28 (4 H, s, C*H*$_2$CO$_2$^{t}Bu) and 3.60 (3 H, s, C*H*$_3$). δ_C (75.43 MHz; $CDCl_3$; TMS) 24.56 (δ*C*H$_2$), 26.02 (β*C*H$_2$), 26.66 (γ*C*H$_2$), 28.10 (C(*C*H$_3$)$_3$), 33.80 (α*C*H$_2$), 51.40 (*C*H$_3$), 53.98 (*en*), 54.83 (*en*), 57.33 (ε*C*H$_2$), 59.27 (*C*H$_2$CO$_2$ ^{t}Bu), 80.83 (*C*(CH$_3$)$_3$), 171.60 (CH$_2$*C*O$_2$ ^{t}Bu) and 173.92 (*C*O$_2$CH$_3$). HRMS (ESI$^+$) calculated for $C_{25}H_{48}N_3O_6$ $(M+H)^+$ 486.35431. Found 486.35278.

NODAHA

A solution of NaOH 1M (7.5 mL) was added to a solution of **NODA(^{t}Bu)HA(me)** (0.225 g, 0.483 mmol) in methanol (2.5 mL). The reaction was left at reflux overnight. The mixture was neutralized with 2 M HCl and stirred with DOWEX for 5 h. The compound was removed with 0.1 M HCl and the solvent evaporated under reduced pressure to give **NODAHA** (0.218 g, 0.464 mmol), as an oil, in a 96% yield. δ_H (400 MHz; D_2O; DSS) 1.53 (2 H, m, γC*H*$_2$), 1.77 (2 H, m, βC*H*$_2$), 1.93 (2 H, m, δC*H*$_2$), 2.54 (2 H, t, *J* = 7.6 Hz, αC*H*$_2$), 3.44-3.75 (14 H, m, εC*H*$_2$ and *en*), 3.94 (4 H, s, C*H*$_2$CO$_2$H). δ_C (100.61 MHz; D_2O; DSS) 23.47 (δ*C*H$_2$), 23.78 (β*C*H$_2$), 25.29 (γ*C*H$_2$), 33.71 (α*C*H$_2$), 49.99 (*en*), 50.77 (en), 51.09 (en), 57.84 (ε*C*H$_2$), 58.12 (*C*H$_2$CO$_2$H), 174.29 (*C*O$_2$H) and

178.93 (CH_2CO_2H). HRMS (ESI^+) calculated for $C_{16}H_{30}N_3O_6$ $(M+H)^+$ 360.21346. Found 360.21279.

Potentiometric studies

Carbonate-free 0.1 M KOH and 0.1 M HCl were prepared from Fisher Chemicals concentrates. Potentiometric titrations were performed in 0.1 M aqueous KCl under nitrogen atmosphere and the temperature was controlled to ± 0.1 °C with a circulating water bath. The p[H] (p[H] = -log[H^+], concentration in molarity) was measured in each titration with a combined pH glass electrode (Metrohm) filled with 3 M KCl and the titrant addition was automated by use of a 702 SM titrino system (Metrohm). The electrode was calibrated in hydrogen ion concentration by titration of HCl with KOH in 0.1 M electrolyte solution [57]. A plot of meter reading versus p[H] allows the determination of the electrode standard potential (E°) and the slope factor (f). Continuous potentiometric titrations with HCl and KOH 0.1 M were conducted on aqueous solutions containing 5 mL of **NODABA** 1.55 mM, 5 mL of **NODAHA** 1.34 mM, and 5 mL of **NODAHep** 3.08 mM in KCl 0.1 M, with 2 minutes waiting between successive points. The titrations of the metal complexes were performed with the same ligand solutions containing 1 equivalent of metal cation, with 2 minutes waiting time between 2 points. Experimental data were refined using the computer program Hyperquad 2008 [58]. All equilibrium constants are concentration quotients rather than activities and are defined as:

$$K_{mlh} = \frac{[M_m L_l H_h]}{[M]^m [L]^l [H]^h} \qquad (7)$$

The ionic product of water at 298 K and 0.1 M ionic strength is pK_w = 13.77 [48]. Fixed values were used for pK_w, ligand acidity constants and total concentrations of metal,

ligand and acid. All values and errors (one standard deviation) reported are at least the average of two consistent and independent experiments.

^{1}H NMR Titrations

Stock solutions of **NODAHep** (11.24 mM), **NODABA** (10.92 mM), and **NODAHA** (10.15 mM) were prepared by dissolving the free chelator in D_2O. The solution was titrated by addition of small aliquots of 0.1 M NaOD or DCl solutions. The final pH was corrected for the deuterium isotope effect using the equation pH = pD - 0.4 [59]. Plots of chemical shifts versus solution pH originated the acid-base titration curves.

Critical micellar concentration determination

Determination by fluorescence

A 40.5 mM stock solution of **[Mn(NODAHep)]** was prepared in 0.1 M HEPES buffer pH 7.4. This concentration was close to the limit of solubility of the chelate. The estimation of the critical micellar concentration (cmc) was performed using ANS (8-anilino-1-naphtalene sulfonic acid) as fluorescence probe [44]. The solutions used in this study were prepared by dilution of the stock solution and each one contained $1x10^{-5}$ M ANS. The fluorescence was measured at 480 nm upon excitation at 350 nm at room temperature. The fluorescence measurements were recorded on a Bio-Tek® Synergy™ HT spectrofluorimeter using the software KC4™.

Relaxometric measurements

A 41.34 mM stock solution of **[Mn(NODAHep)]** was prepared; by dilution it was possible to have a set of solutions in the concentration range 4.68 mM - 41.34 mM in 0.5 M HEPES buffer pH 7.4, whose relaxivity was measured at 40 MHz and 298 K.

^{1}H NMRD studies

Proton NMRD (nuclear magnetic relaxation dispersion) profiles were recorded on a Stelar SMARtracer Fast Field Cycling NMR relaxometer (0.01-10 MHz) and a Bruker

WP80 NMR electromagnet adapted to variable field measurements and controlled by a SMARtracer PC-NMR console. The temperature was monitored by a VTC91 temperature control unit and maintained by a gas flow. The temperature was determined by previous calibration with a Pt resistance temperature probe. The longitudinal relaxation rates ($1/T_1$) were determined in water. The least-square fit of the ^{1}H NMRD data were performed by using MicroMath Scientist version 2.0 (Salt Lake City, UT, USA). The concentrations and pH of solutions were as follows: **[Mn(NODAHep)]** 4.68 mM; **[Mn(NODABA)]** 4.40 mM and **[Mn(NODAHA)]** 5.70 mM in 0.5 M HEPES buffer pH 7.4. The ^{1}H NMRD profiles were obtained at 298, 310 and 323 K. HRMS (ESI^+): **[Mn(NODAHep)]** – calculated for $C_{17}H_{32}MnN_3O_4$ $(M+H)^+$ 397.1773. Found 397.1761; **[Mn(NODABA)]** – calculated for $C_{18}H_{24}MnN_3O_6$ $(M+H)^+$ 433.1046. Found 433.1039; **[Mn(NODAHA)]** – calculated for $C_{16}H_{28}MnN_3O_6$ $(M+H)^+$ 413.1359. Found 413.1350.

^{17}O NMR studies

The longitudinal and transverse ^{17}O relaxation rates ($1/T_{1,2}$) and the chemical shifts were measured in aqueous solutions of the various complexes in the temperature range 280-350 K, on a Bruker Avance 500 (11.7 T, 67.8 MHz) spectrometer. The temperature was calculated according to previous calibration with ethylene glycol and methanol [60]. An acidified water solution ($HClO_4$, pH 3.3) was used as external reference. Transverse relaxation times (T_2) were obtained by the Carr-Purcell-Meiboom-Gill spin-echo technique [61] and longitudinal relaxation times were measured by the inversion recovery sequence [62]. The technique of the ^{17}O NMR measurements on Gd^{3+} complexes has been described elsewhere [63]. The samples were sealed in glass spheres fitted into 10 mm NMR tubes to avoid susceptibility corrections of the chemical shifts [64]. To improve the sensitivity, ^{17}O-enriched water (10% $H_2{}^{17}O$, CortectNet) was added to the solutions to

reach around 1% enrichment. The complex solutions were prepared in 0.5 M HEPES buffer at pH 7, and the concentrations were as follows: **[Mn(NODAHep]** = 4 mM; **[Mn(NODAHA)]** = 4.04 mM; **[Mn(NODABA)]** = 4.00 mM. The ^{17}O NMR data have been treated according to the Solomon-Bloembergen-Morgan theory of paramagnetic relaxation [65] (see Supporting Information). The least-squares fit of the ^{17}O NMR data were performed using Micromath Scientist version 2.0 (Salt Lake City, UT, USA). The reported errors correspond to two times the standard deviation.

Interaction with HSA

A Solution of **[Mn(NODAHep)]** (4.68 mM) and HSA (0.607 mM) was prepared in 0.5 M HEPES buffer pH 7.4. The ^{1}H NMRD profile was obtained at 298 K.

pH stability range

Solutions of **[Mn(NODAHep)]** (1 mM) were prepared in the pH range 1.72 - 9.25. The longitudinal relaxation rates were measured at 20 MHz and 298 K. The measurements were carried out in a BrukerMinispec MQ 20.

Abbreviations

AAZTA = 6-amino-6-methylperhydro-1,4-diazepine triacetic acid

ANS = 8-anilino-1-naphtalene sulfonic acid

BOM = benzyloxymethyl

cmc = critical micellar concentration

CAs = contrast agents

COSY = correlation spectroscopy

d = duplet

DCM = dichloromethane

diph = diphenylcyclohexylphosphate

DO2A = 1,4,7,10-tetraazacyclododecan-1,7-diacetic acid

DO3A = 1,4,7,10-tetraazacyclododecane-1,4,7-triacetic acid

DOTA = 1,4,7,10-tetraazacyclododecane-1,4,7,10-tetraacetate

DOTAM = 1,4,7,10-tetraazacyclododecane-1,4,7,10-tetraacetamide

DPDP = *N,N'*-dipyridoxylethylenediamine-*N,N'*-diacetate-5,5'-bis-(phosphate)

DSS = sodium 2,2-dimethylsilapentane-5-sulfonate

DTPA = diethylenetriaminepentaacetate

EDTA = ethylenediamine tetraacetic acid

en = ethylenic bridges

ENOTA = dimeric triazacyclononane-based ligand

ESI^+ = positive electrospray ionization

Fm = 9-fluorenylmethyl

HEPES = 4-(2-hydroxyethyl)-1-piperazineethanesulfonic acid

HRMS = high-resolution mass spectrometry

HSA = Human serum albumin

m = multiplet

MeCN = acetonitrile

MeOH = methanol

MRI = magnetic resonance imaging

NMR = nuclear magnetic resonance

NMRD = nuclear magnetic relaxation dispersion

NO2AtBu = 1,4,7-triazacyclononane-1,4-diacetic acid *tert*-butyl ester

NODABA = 1,4,7-triazacyclononane-1,4-diacetate-7-benzoic acid

NODAHA = 1,4,7-triazacyclononane-1,4-diacetate-7-hexanoic acid

NODAHep = 1,4,7-triazacyclononane-1,4-diacetate-7-heptanil

NOTA = 1,4,7-triazacyclononane-1,4,7-triacetate

NOTAC8 = 1,4,7-triazacyclononane-1,4-diacetic acid-7-octanoic acid-

s = singlet

SBM = Solomon-Bloembergen-Morgan

t = triplet

TFA = trifluoracetic acid

TLC = thin layer chromatography

TMS = tetramethylsilane

Acknowledgements

We thank the financial support from Fundação para a Ciência e a Tecnologia (F.C.T.), Portugal and Fundo Social Europeu (FSE) (PhD grant SFRH/BD/63639/2009 and Rede Nacional de RMN (REDE/1517/RMN/2005) for the acquisition of the Bruker Avance III 400 NMR spectrometer at the University of Minho), as well as financial support from La Ligue Contre le Cancer, France (E. T.). This work was carried out in the frame of the COST Actions D38 "Metal Based Systems for Molecular Imaging" and TD1004 "Theragnostics Imaging and Therapy"

Supplementary Information. Figure S1. Determination of cmc of **[Mn(NODAHep)]** by paramagnetic relaxation enhancement measurements. Figure S2. Potentiometric titration curves of solutions containing **NODAHA** 1.34 mM with 0 or 1 equivalent of Mn^{2+} or Zn^{2+} in H_2O, KCl 0.1 M, 298 K. Figure S3. Potentiometric titration curves of solutions containing **NODABA** 1.55 mM with 0 or 1 equivalent of Mn^{2+} or Zn^{2+} in H_2O, KCl 0.1 M, 298 K. Figure S4. (Top) Temperature dependence of reduced ^{17}O transverse relaxation rate of **[Mn(NODAHA)]**. (Bottom) ^{1}H NMRD profiles of

[Mn(NODAHA)] at 298, 310 and 323 K. Figure S5. (Top) Temperature dependence of reduced ^{17}O transverse relaxation rate of **[Mn(NODABA)]**. (Bottom) ^{1}H NMRD profiles of **[Mn(NODABA)]** at 298, 310 and 323 K. Figure S6. ^{1}H NMRD profile of **[Mn(NODAHep)]** in the presence of HSA at 298 K. Equations used for the analysis of NMRD and ^{17}O NMR data.

References

1. É. Tóth, L. Helm and A. E. Merbach, *Contrast Agents I*, 2002, **221**, 61-101.
2. H. J. Weinmann, R. C. Brasch, W. R. Press and G. E. Wesbey, *Amer. J. Roentgenology*, 1984, **142**, 619-624.
3. M. Magerstädt, O. A. Gansow, M. W. Brechbiel, D. Colcher, L. Baltzer, R. H. Knop, M. E. Girton and M. Naegele, *Magn. Reson. Med.*, 1986, **3**, 808-812.
4. S. M. Rocklage, W. P. Cacheris, S. C. Quay, F. E. Hahn and K. N. Raymond, *Inorg. Chem.*, 1989, **28**, 477-485.
5. T. Murakami, R. L. Baron, M. S. Peterson, J. H. Oliver, P. L. Davis, S. R. Confer and M. P. Federle, *Radiology*, 1996, **200**, 69-77.
6. B. Drahoš, I. Lukeš and É. Tóth, *Eur. J. Inorg. Chem.*, 2012, 1975-1986.
7. S. H. Koenig, C. Baglin and R. D. Brown, *Magn. Reson. Med.*, 1984, **1**, 496-501.
8. J. Maigut, R. Meier, A. Zahl and R. van Eldik, *Inorg. Chem.*, 2008, **47**, 5702-5719.
9. S. Aime, P. L. Anelli, M. Botta, M. Brocchetta, S. Canton, F. Fedeli, E. Gianolio and E. Terreno, *J. Biol. Inorg. Chem.*, 2002, **7**, 58-67.
10. J. S. Troughton, M. T. Greenfield, J. M. Greenwood, S. Dumas, A. J. Wiethoff, J. F. Wang, M. Spiller, T. J. McMurry and P. Caravan, *Inorg. Chem.*, 2004, **43**, 6313-6323.
11. D.-W. Zhang, Z.-Y. Yang, S.-P. Zhang and R.-D. Yang, *Trans. Metal Chem.*, 2006, **31**, 333-336.
12. A. Bertin, J. Steibel, A. I. Michou-Gallani, J. L. Gallani and D. Felder-Flesch, *Bioconjug. Chem.*, 2009, **20**, 760-767.
13. H. A. Tang, Y. Sheng and R. D. Yang, *Inorg. Chem. Commun.*, 2003, **6**, 1213-1216.
14. C. F. C. G. Geraldes, A. D. Sherry, R. D. Brown and S. H. Koenig, *Magn. Reson. Med.*, 1986, **3**, 242-250.
15. E. Balogh, Z. J. He, W. Y. Hsieh, S. Liu and É. Tóth, *Inorg. Chem.*, 2007, **46**, 238-250.
16. B. Drahoš, M. Pniok, J. Havlíčková, J. Kotek, I. Císařová, P. Hermann, I. Lukeš and É. Tóth, *Dalton Trans.*, 2011, **40**, 10131-10146.
17. A. Bianchi, L. Calabi, C. Giorgi, P. Losi, P. Mariani, D. Palano, P. Paoli, P. Rossi and B. Valtancoli, *J. Chem. Soc. Dalton Trans.*, 2001, 917-922.
18. S. Wang and T. D. Westmoreland, *Inorg. Chem.*, 2009, **48**, 719-727.

19. L. Tei, G. Gugliotta, M. Fekete, F. K. Kálmán and M. Botta, *Dalton Trans.*, 2011, **40**, 2025-2032.
20. J. E. Newton and S. C. Jackels, *J. Coord. Chem.*, 1988, **19**, 265-277.
21. S. C. Jackels, M. M. Durham, J. E. Newton and T. C. Henninger, *Inorg. Chem.*, 1992, **31**, 234-239.
22. B. Drahoš, J. Kotek, I. Cí sařová P. Hermann, L. Helm, I. Lukeš and É. Tóth, *Inorg. Chem.*, 2011, **50**, 12785-12801.
23. D. P. Cistola and D. M. Small, *J. Clin. Invest.*, 1991, **87**, 1431-1441.
24. S. Aime, M. Botta, M. Fasano and E. Terreno, *Chem. Soc. Rev.*, 1998, **27**, 19-29.
25. M. Fasano, S. Curry, E. Terreno, M. Galliano, G. Fanali, P. Narciso, S. Notari and P. Ascenzi, *IUBMB Life*, 2005, **57**, 787-796.
26. S. Aime, M. Botta, M. Fasano, S. G. Crich and E. Terreno, *J. Biol. Inorg. Chem.*, 1996, **1**, 312-319.
27. S. M. Moghimi, A. C. Hunter and J. C. Murray, *Pharmacol. Rev.*, 2001, **53**, 283-318.
28. V. P. Torchilin, A. N. Lukyanov, Z. Gao and B. Papahadjopoulos-Sternberg, *Proc. Natl. Acad. Sci. U.S.A.*, 2003, **100**, 6039-6044.
29. J. Wang, D. Mongayt and V. P. Torchilin, *J. Drug Target.*, 2005, **13**, 73-80.
30. K. Kostarelos and D. Emfietzoglou, *J. Liposome Res.*, 1999, **9**, 429-460.
31. P. C. Griffiths, I. A. Fallis, T. Chuenpratoom and R. Watanesk, *Adv. Colloid Interface Sci.*, 2006, **122**, 107-117.
32. W. J. Mulder, G. J. Strijkers, G. A. van Tilborg, A. W. Griffioen and K. Nicolay, *NMR Biomed.*, 2006, **19**, 142-164.
33. G. M. Lanza, P. M. Winter, M. S. Hughes, S. D. Caruthers, J. N. Marsh, A. M. Morawski, A. H. Schmieder, M. J. Scott, R. W. Fuhrhop, H. Zhang, G. Hu, E. K. Lacy, J. S. Allen and S. A. Wickline, in *Polymeric Drug Delivery I*, ed. S. Svenson, American Chemical Society, 2006, vol. 923, pp. 295-311.
34. R. Hovland, C. Gløgård, A. J. Aasen and J. Klaveness, *Org. Biomol. Chem.*, 2003, **1**, 644-647.
35. B. Misselwitz, J. Platzek, B. Radüchel, J. J. Oellinger and H. J. Weinmann, *Magnetic Resonance Materials in Physics, Biology and Medicine*, 1999, **8**, 190-195.
36. J. P. André, É. Tóth, H. Fischer, A. Seelig, H. R. Mäcke and A. E. Merbach, *Chem. Eur. J.*, 1999, **5**, 2977-2983.
37. M. Schottelius and H. J. Wester, *Methods*, 2009, **48**, 161-177.
38. D. D. Castelli, E. Gianolio, S. G. Crich, E. Terreno and S. Aime, *Coord. Chem. Rev.*, 2008, **252**, 2424-2443.
39. A. H. Schmieder, P. M. Winter, S. D. Caruthers, T. D. Harris, T. A. Williams, J. S. Allen, E. K. Lacy, H. Y. Zhang, M. J. Scott, G. Hu, J. D. Robertson, S. A. Wickline and G. M. Lanza, *Magn. Reson. Med.*, 2005, **53**, 621-627.
40. S. Liu and D. S. Edwards, in *Contrast Agents II*, ed. W. Krause, Springer, 2002, vol. 222, pp. 259-278.
41. P. Caravan, J. J. Ellison, T. J. McMurry and R. B. Lauffer, *Chem. Rev.*, 1999, **99**, 2293-2352.
42. J. P. André, C. F. C. G. Geraldes, J. A. Martins, A. E. Merbach, M. I. M. Prata, A. C. Santos, J. J. P. de Lima and É. Tóth, *Chem.--Eur. J.*, 2004, **10**, 5804-5816.
43. K. S. Birdi, H. N. Singh and S. U. Dalsager, *J. Phys. Chem.*, 1979, **83**, 2733-2737.
44. E. De Vendittis, G. Palumbo, G. Parlato and V. Bocchini, *Anal. Biochem.*, 1981, **115**, 278-286.

45. A. Morisco, A. Accardo, E. Gianolio, D. Tesauro, E. Benedetti and G. Morelli, *J. Pept. Sci.*, 2009, **15**, 242-250.
46. A. de Sá, M. I. M. Prata, C. F. G. C. Geraldes and J. P. André, *J. Inorg. Biochem.*, 2010, **104**, 1051-1062.
47. C. F. G. C. Geraldes, M. C. Alpoim, M. P. M. Marques, A. D. Sherry and M. Singh, *Inorg. Chem.*, 1985, **24**, 3876-3881.
48. R. M. Smith, R. J. Motekaitis and A. E. Martell, *NIST Standard Reference Database*, National Institute of Standards and Technology, 1997.
49. S. Cortes, E. Brücher, C. F. C. G. Geraldes and A. D. Sherry, *Inorg. Chem.*, 1990, **29**, 5-9.
50. B. Drahos, J. Kotek, P. Hermann, I. Lukes and E. Toth, *Inorg Chem*, 2010, **49**, 3224-3238.
51. R. M. Smith, R. J. Motekaitis and A. E. Martell.
52. P. H. Fries and E. Belorizky, *J. Chem. Phy.*, 2005, **123**, 124510.
53. Y. Ducommun, K. E. Newman and A. E. Merbach, *Inorg. Chem.*, 1980, **19**, 3696-3703.
54. J. Maigut, R. Meier, A. Zahl and R. v. Eldik, *Journal of the American Chemical Society*, 2008, **130**, 14556-14569.
55. É. Tóth and A. E. Merbach, *The Chemistry of Contrast agents in Medical Magnetic Resonance Imaging*, John Wiley & Sons, Chichester, 2001.
56. V. Henrotte, L. Vander Elst, S. Laurent and R. N. Muller, *J. Biol. Inorg. Chem.*, 2007, **12**, 929-937.
57. A. E. Martell and R. J. Motekaitis, *Determination and Use of Stability Constants*, Wiley-VCH, 1992.
58. P. Gans, A. Sabatini and A. Vacca, *Talanta*, 1996, **43**, 1739-1753.
59. K. Mikkelsen and S. O. Nielsen, *J. Phys. Chem.*, 1960, **64**, 632-637.
60. D. S. Raiford, C. L. Fisk and E. D. Becker, *Anal. Chem.*, 1979, **51**, 2050-2051.
61. S. Meiboom and D. Gill, *Rev. Sci. Instrum.*, 1958, **29**, 688-691.
62. R. L. Vold, J. S. Waugh, M. P. Klein and D. E. Phelps, *J. Chem. Phys.*, 1968, **48**, 3831-3832.
63. K. Micskei, L. Helm, E. Brücher and A. E. Merbach, *Inorganic Chemistry*, 1993, **32**, 3844-3850.
64. A. D. Hugi, L. Helm and A. E. Merbach, *Helv. Chim. Acta*, 1985, **68**, 508-521.
65. É. Tóth, L. Helm and A. E. Merbach, in *The Chemistry of Contrast agents in Medical Magnetic Resonance Imaging*, eds. A. E. Merbach and É. Tóth, Wiley, 2001.

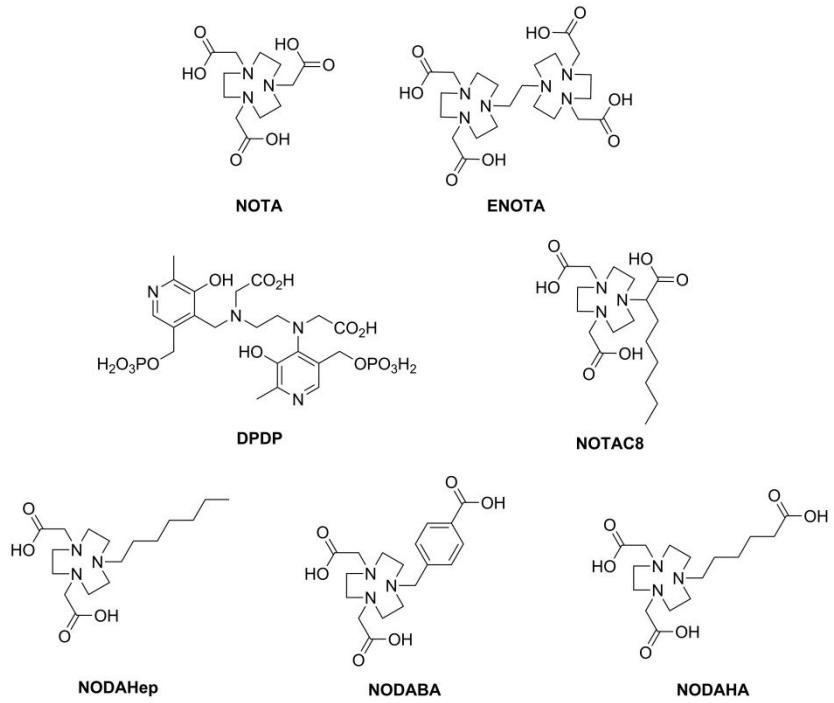

Scheme 1. Chemical structure of various chelators for Mn^{2+} discussed in this work.

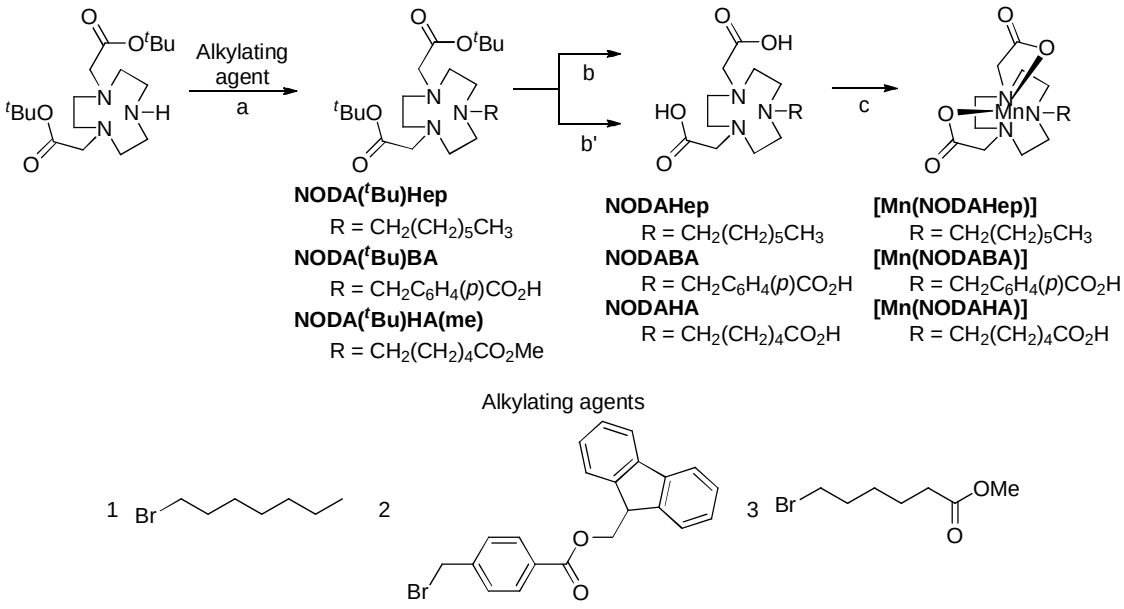

Scheme 2. a: K_2CO_3 in MeCN; b: TFA in DCM; b': 1 M NaOH in MeOH, Δ; c: $MnCl_2.4H_2O$ in 0.5 M HEPES buffer, pH 7.4.

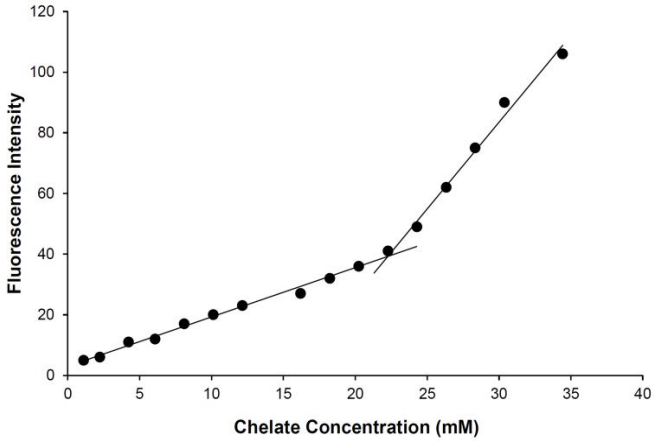

Figure 1. Determination of cmc by fluorescence spectroscopy. The intersection of the linear regression curves of the fluorescence intensity of ANS at 480 nm as a function of the chelate concentration determines the cmc of **NODAHep**.

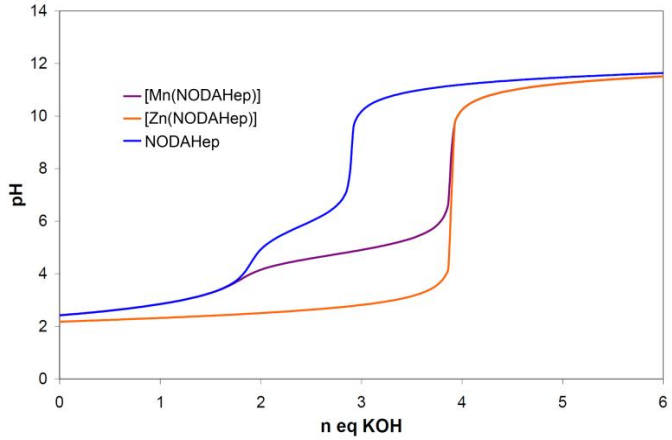

Figure 2. Potentiometric titration curves of solutions containing **NODAHep** 3.08 mM with 0 or 1 equivalent of Mn^{2+} or Zn^{2+} in H_2O, KCl 0.1 M, 298 K.

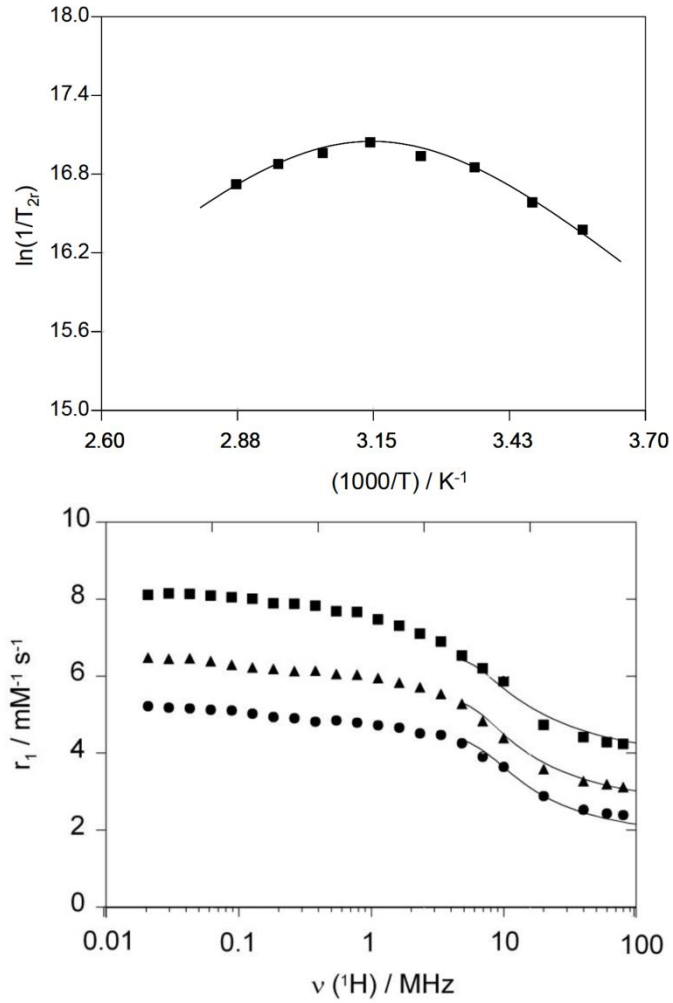

Figure 3. (Top) Temperature dependence of reduced ^{17}O transverse relaxation rate of **[Mn(NODAHep)]**. (Bottom) ^{1}H NMRD profiles of **[Mn(NODAHep)]** at 298 K (■), 310 K (▲), and 323 K (●).

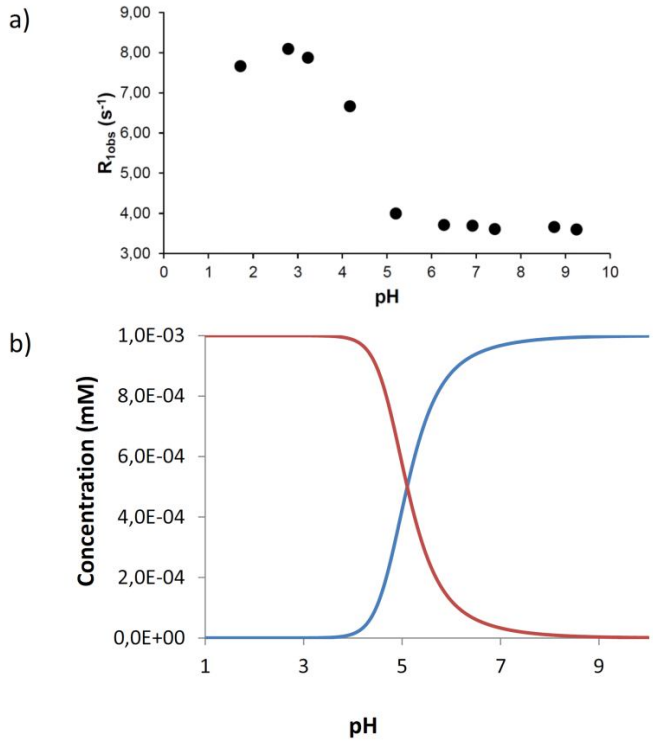

Figure 4. Stability of **[Mn(NODAHep)]** as a function of the pH: a) Paramagnetic relaxation enhancement measured at 1 mM, 20 MHz, and 298 K. b) Species distribution obtained in the same conditions from the stability constants (Table 1 and 2).

Table 1. Protonation constants of various ligands at 298 K and in KCl = 0.1 M.

	NODAHep	**NODAHA**	**NODABA**	**NOTA**
Log K_{H1}	12.0(3)	11.1(2)	11.2(1)	11.41
Log K_{H2}	5.81(2)	6.00(5)	5.35(3)	5.74
Log K_{H3}	2.71(8)	4.53(2)	4.07(6)	3.16
Log K_{H4}		2.74(5)	3.04(9)	1.71
Log K_{H5}			2.0(1)	

Table 2. Stability constants, and pM values of **NODAHep**, **NODAHA**, **NODABA**, and NOTA complexes with Mn^{2+} and Zn^{2+} ions at 298 K, and in KCl 0.1 M.

Log *K*	**NODAHep**	**NODAHA**	**NODABA**	**NOTA**[a]
MnL	10.98(3)	10.15(5)	9.9(1)	14.9
MnLH		4.95(5)		
MnLOH		9.65(5)		
ZnL	16.6(1)	15.65(7)	15.72(9)	18.6
ZnLH		4.76(2)	4.25(8)	
$ZnLH_2$			2.52(7)	
% free Mn^{2+} [b]	0.92	0.85	1.26	$7.8x10^{-3}$
pMn[c]	7.35	7.41	7.09	11.8

a. From ref [48, 49]. b. obtained at pH = 7.4 for [Mn] = [L] = 5 mM. c. $pMn = - \log [Mn]_{free}$ for pH = 7.4, [Mn] = 10^{-6} M, [L] = 10^{-5} M.

Table 3. Best fit parameters obtained from the simultaneous analysis of ^{17}O NMR and ^{1}H NMRD data.

	MnNODAHep	**MnNODAHA**	**MnNODABA**	**Mn_2ENOTA**[a]	**$Mn(H_2O)_6$**[b]
k_{ex}^{298}($10^6 s^{-1}$)	2.7 (2)	2.7 (2)	1.3 (3)	5.5	2.1
$\Delta H^{\neq}$(kJ.mol^{-1})	23.4 (9)	23.5 (9)	10.9 (9)	20.5	32.9
$\Delta S^{\neq}$(J.mol^{-1}.K^{-1})	- 24 (2)	- 24 (2)	- 72 (4)	- 28	+ 5.7
E_R (kJ.mol^{-1})	25 (1)	24 (1)	27(1)	18	
τ_{RO}^{298}(ps)	84 (1)	80 (1)	121 (6)	85	
τ_v^{298}(ps)	60 (5)	69 (9)	60[c]	7.7	3.3
Δ^2($10^{18} s^{-1}$)	70 (1)	70 (1)	70[c]	4.7	5.6
$A_0/\hbar$(10^6rad.s^{-1})	30 (1)	30 (1)	33 (1)	32.7	33.3

[a] From ref [15]. [b] From ref [53]. [c] These values have been fixed for the fitting (see text).